Spatiotemporal Chaotic Localized State in Liquid Crystal Light Valve Experiments with Optical Feedback

N. Verschueren,[1] U. Bortolozzo,[2] M. G. Clerc,[1] and S. Residori[2]

[1]*Departamento de Física, FCFM, Universidad de Chile, Casilla 487-3, Santiago, Chile*

[2]*INLN, Université de Nice-Sophia Antipolis, CNRS, 1361 route des Lucioles, 06560 Valbonne, France*

(Received 4 October 2012; published 5 March 2013)

The existence, stability properties, and dynamical evolution of localized spatiotemporal chaos are studied. We provide evidence of spatiotemporal chaotic localized structures in a liquid crystal light valve experiment with optical feedback. The observations are supported by numerical simulations of the Lifshitz model describing the system. This model exhibits coexistence between a uniform state and a spatiotemporal chaotic pattern, which emerge as the necessary ingredients to obtain localized spatiotemporal chaos. In addition, we have derived a simplified model that allows us to unveil the front interaction mechanism at the origin of the localized spatiotemporal chaotic structures.

DOI: 10.1103/PhysRevLett.110.104101 PACS numbers: 05.45.−a, 05.45.Jn, 05.45.Pq, 89.75.Kd

Out of equilibrium macroscopic systems are characterized by exhibiting self-structuring phenomena [1–3]. In the course of recent decades, much effort has been devoted to study pattern formation in diverse branches of natural sciences (see, e.g., Refs. [4–6] and references therein). In most of the systems it has been observed the emergence of localized states [7–12], which, although being spatially extended, exhibit properties associated with particlelike states, such as position and width. In one-dimensional spatial systems, localized states can be described as spatial trajectories that connect one steady state with itself, which means they are homoclinic orbits from the point of view of dynamical systems [13]. Particular types of localized states are localized patterns, which correspond to patterns extended only over a small portion of a spatial system [1,3]. A geometrical interpretation of the existence, stability properties, and bifurcation diagram of localized patterns in one-dimensional extended systems has been proposed in Refs. [14,15]. Recently, the existence of localized patterns based on front interaction was developed [16]. Consequently, one could imagine localized states of different types supported by different states, for example, a pattern over a pattern [17], an oscillatory state over a uniform one [18], or a wave over a uniform state [19]. In the case of a localized oscillatory state, it has been shown that if one increases the amplitude of the forcing, the amplitude of the breather undergoes a double-period route to chaos, hence realizing a low dimensional localized chaotic state [18]. A similar route has been observed for discrete breathers in anisotropic Josephson junction ladders [20]. Chaotic localized states have also been reported in models of heterogeneous catalytic reaction in porous particles [21], whereas localized chaotic domains were observed in surface wave experiments as a result of the curvature of the container walls [22]. Notwithstanding, the above scenario is incomplete, as one would expect to find situations where it is possible to obtain localized states characterized by spatiotemporal chaotic dynamics developing over a uniform state. To our knowledge, there is, to date, no observation or theory of this type of localized state.

The purpose of this Letter is to provide evidence of the existence, stability properties, and dynamical evolution of localized spatiotemporal chaos. Experimentally, this type of localized state are observed in a liquid crystal light valve (LCLV) experiment with feedback loop. Figure 1 shows an example of the observed spatiotemporal chaotic localized state and its respective spatiotemporal evolution. Close to the nascent of bistability and spatial bifurcation, the Lifshitz point [3], a generalization of the variational

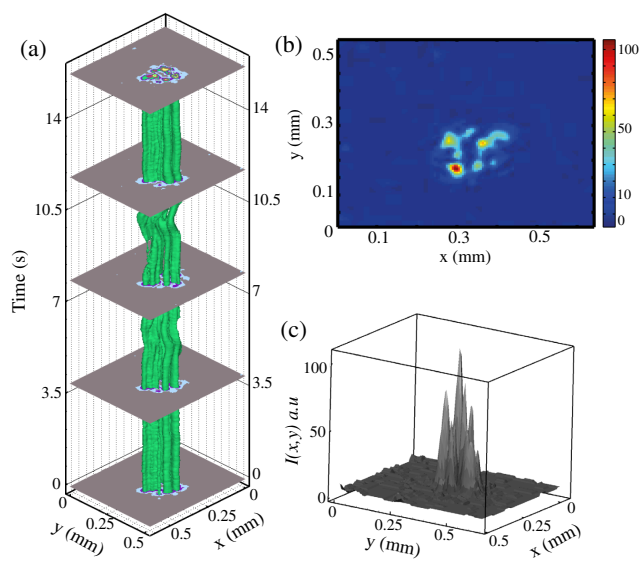

FIG. 1 (color online). Chaoticon structure observed in the LCLV experiment. (a) Temporal evolution of the light intensity isosurface; the camera acquisition rate is 30 fps. (b) Instantaneous snapshot. (c) Plot of the light intensity at a given time.

 © 2013 American Physical Society

Swift-Hohenberg equation—*the Lifshitz normal form*—describes this system [23]. For a certain region of parameters, this model exhibits coexistence between a uniform state and a chaotic spatiotemporal pattern, which are the necessary ingredients to have spatiotemporal chaotic localized states, that we term *chaoticons*. When increasing the size of the localized structures, a transition from the stationary to the spatiotemporal chaotic states is observed, consistent with the fact that, as one increases the size of localized states, additional modes are incorporated in the dynamics. In order to reveal the livelihood mechanism of these states, we also buildup a phenomenological prototype bistable model forced with a spatiotemporal chaotic source. This allows us to analytically characterize the pinning front interaction between a uniform and a spatiotemporal chaotic state.

Experimental evidence of chaoticons.—We consider a LCLV experiment, which is composed of a nematic liquid crystal (LC) film sandwiched in between a glass and a photoconductive plate over which a dielectric mirror is deposited (for details see, e.g., the review [24]). The LC film has a planar aligned nematic director $\vec{n}$ parallel to the walls, with a thickness $d = 15\ \mu$m. The liquid crystal is a mixture of cyano-biphenyls (nematic LC-654, produced by NIOPIK), with a dielectric anisotropy $\Delta\varepsilon \equiv \varepsilon_{\parallel} - \varepsilon_{\perp} = 10.7$ and optical birefringence, $\Delta n \equiv n_{\parallel} - n_{\perp} = 0.2$, where $\varepsilon_{\parallel}$ and $\varepsilon_{\perp}$ are the dielectric permittivities $\parallel$ and $\perp$ to $\vec{n}$, respectively, and $n_{\parallel}$ and are $n_{\perp}$ are the extraordinary ($\parallel$ to $\vec{n}$) and ordinary ($\perp$ to $\vec{n}$) refractive index, respectively. Transparent electrodes over the glass plates permit the application of an electrical voltage across the LC layer, which allows applying a reference voltage V_0 without feedback. The photoconductor behaves like a variable resistance, decreasing for increasing illumination. The feedback is obtained by sending back onto the photoconductor the light which has passed through the LC layer and has been reflected by the dielectric mirror [24]. This light beam experiences a phase shift which depends on the liquid crystal reorientation and, on its turn, modulates the effective voltage that locally applies to the LC layer. The optical free propagation length in the feedback loop is fixed to $L = -4.0$ cm. This parameter, together with the laser wavelength λ, controls the characteristic size of the optical patterns [24].

For a fixed voltage V_0, by increasing the laser intensity the system presents a bistability between a spatiotemporal complex pattern and a homogeneous state. In order to carefully identify the bistability region, an acousto-optic modulator is placed on the optical path of the input beam and allows changing the intensity of the light impinging onto the LCLV. Figure 2 illustrates the experimental bifurcation diagram obtained by decreasing the laser intensity $I_{\rm in}$ with respect to a reference value $I_0 = 1.6$ mW/cm^2 at a fixed voltage $V_0 = 8.12$ V rms. In the coexistence region, by making a local perturbation with a low power external

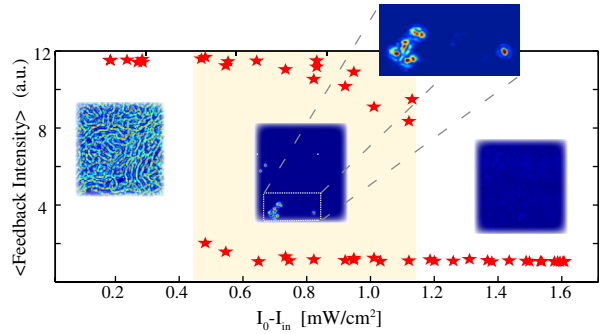

FIG. 2 (color online). Bifurcation diagram of states observed in the LCLV experiment; the average pattern intensity is plotted versus the input laser intensity $I_{\rm in}$; the upper and lower branches correspond to the spatiotemporal chaotic pattern and uniform state, respectively. Insets display example pictures of observations in the respective regions. The shaded area represents the coexistence region. An enlarged view of the chaoticon is shown in the upper central inset.

beam, by using a digital light processing projector, we can induce localized structures of different size from the uniform state. Once created, the localized structures remain stable when removing the external beam. By changing the position of the initial perturbation, the localized structure can be spatially addressed and generated in any space position over the photoconductor area. The central inset of Fig. 2 shows an example of induced structures. As a first observation, we note that localized structures that are transversally small (formed by 1 or 2 elementary cells, each cell being one of the peaks composing the structure) are stationary. When the localized structures become larger (composed at least by 5 or 6 elementary cells), they exhibit a complex spatiotemporal behavior, realizing a chaoticon structure as the one in the example shown in Fig 1.

Theoretical description.—In order to establish a theoretical basis supporting the observations, we resort to the one-dimensional Lifshitz normal form that describes the LCLV system close to the point of nascent bistability and spatial bifurcation [23]

$$\partial_t u = -\eta + \mu u - u^3 + \nu \partial_{xx} u - \partial_{xxxx} u + b u \partial_{xx} u + c(\partial_x u)^2, \quad (1)$$

where $u(x, t)$ is a scalar field proportional to the average tilt angle of the liquid crystal molecules, μ is the bifurcation parameter, η accounts for the asymmetry between homogeneous states, c is the nonlinear advection coefficient, and $\{\nu, b\}$ are, respectively, the linear and nonlinear diffusion coefficients. The relation of these parameters with the physical parameters is given in Ref. [25]. Equation (1) has also been derived in the context of biological systems, optical cavities and chemical reactions [26], which emphasizes its universal nature. For $b = c = \eta = 0$ it corresponds to the well-known Swift-Hohenberg (SH) model [3,5], whose dynamics is characterized by the

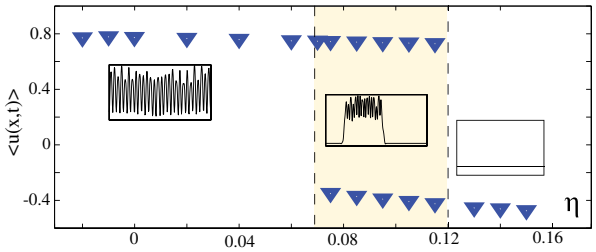

FIG. 3 (color online). Bifurcation diagram of the Lifshitz model, Eq. (1), $\mu = -0.09$, $\nu = -1$, $b = -3.5$, $c = 10$. The upper and lower branches correspond to the spatiotemporal chaotic pattern and uniform state, respectively. The insets display pattern profiles obtained in the respective regions. The shaded area represents the coexistence region.

minimization of a functional energy. Contrarily, Eq. (1) is of nonvariational type; therefore, one expects that model (1) exhibits permanent dynamics as oscillations, propagations and spatiotemporal chaos. For negative diffusion ($\nu < 0$), the SH equation exhibits stationary patterns in a wide range of parameters [3,5]. Contrarily, when increasing c, Eq. (1) exhibits permanent dynamical behaviors of the patterns, with a route from stationary to spatiotemporal chaotic patterns [27]. Furthermore, the spatiotemporal chaotic patterns have a coexistence region with the uniform state, as illustrated in Fig. 3.

The experimental bifurcation diagram (Fig. 2) and the one calculated from the model (1) (Fig. 3) share the same qualitative behavior. However, experimental observations close to the Lifshitz point are a complex task because fluctuations and inhomogeneities play an important role in the observed dynamics. Therefore, experiments are carried away from the Lifshitz point and the theoretical and experimental likeness presented here has to be considered only as a qualitative and not a quantitative one. In analogy with the experimental observations, we expect to obtain *chaoticons* in the region of coexistence between the uniform state and the spatiotemporal chaotic pattern. Indeed, numerical simulations of model (1) exhibit localized spatiotemporal states that become chaotic when the size of the structures is large enough. Figures 4(a)–4(d) displays spatiotemporal localized states with different cell numbers. We use the term cells as the number of maxima on the localized state. For each of them the respective largest Lyapunov exponent was calculated with standard methods as described in Refs. [28]. The exponent obtained with both the methods was the same and it is plotted in Fig. 4(g). Figures 4(e) and 4(f) show typical temporal evolutions of the respective field u at two given points. The small localized structures are steady states with negative largest Lyapunov exponent. Then, starting from a critical size, the localized states exhibit complex spatiotemporal dynamics and, eventually, become characterized by a positive Lyapunov exponent. The spatiotemporal chaos observed for these cases can be understood as a consequence of an

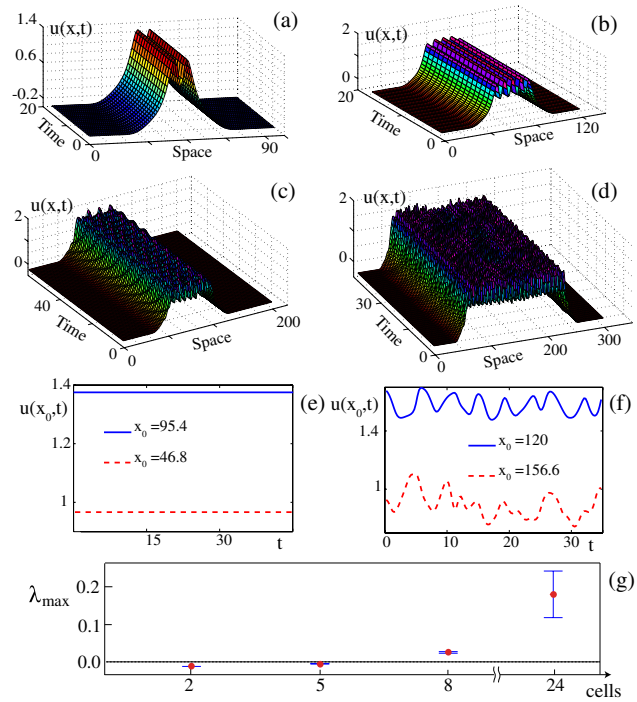

FIG. 4 (color online). Spatiotemporal diagrams of localized structures of model (1), $\mu = -0.09$, $\nu = -1$, $b = -3.5$, $\eta = 0.04$, $c = 10$, for (a) 2, (b) 5, (c) 8, and (d) 24 cells using 512 points in space ($dx = 0.5$) and a temporal step $dt = 0.01$. Temporal evolutions of u at two given points for (e) 2 and (f) 24 cells. (g) The largest Lyapunov exponent versus the number of cells.

increased number of spatial modes participating to form larger structures, the interaction of these modes being responsible for the complex behaviors. Indeed, if one continues to increase the size of the localized states, the Lyapunov exponent increases slightly while more modes are incorporated into the permanent dynamics. These behaviors are consistent with the experimental observations.

In order to shed light into the livelihood mechanism that support the chaoticon structures and to understand their nature as the result of front interaction [13,16], we have built up a simplified phenomenological model in which we insert *ad hoc* the minimal ingredients, namely, the coexistence between a uniform state and a chaotic spatiotemporal pattern with controlled amplitude. For this, we consider the Nagumo-Kuramoto (NK) model

$$\partial_t u = u(u-1)(\alpha - u) + \partial_{xx} u + u\cos(kx)(\beta + \gamma \partial_x \Psi), \tag{2}$$

$$\partial_t \Psi = (\partial_x \Psi)^2 - \partial_{xx}\Psi - \partial_{xxxx}\Psi. \tag{3}$$

For $\beta = \gamma = 0$, the field $u(x,t)$ satisfies the Nagumo model, Eq. (2), used to describe front propagation in population dynamics [29]. Here, α controls the relative

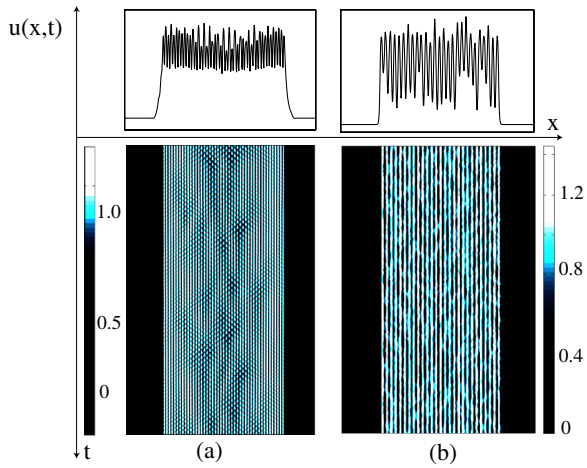

FIG. 5 (color online). Numerical observations of chaoticons and respective spatiotemporal diagrams in (a) the Lifshitz model, Eq. (1), $\mu = -0.09$, $\nu = -1$, $b = -3.87$, $\eta = 0.04$, $c = 10$ and (b) the phenomenological Nagumo-Kuramoto model, Eqs. (2) and (3), $\alpha = 0.5$, $\beta = 0.3$, $k = 11$, $\gamma = 0.3$.

stability between the two equilibria ($u = 0$ and $u = 1$), while the term proportional to β is responsible for the change of the uniform state, $u = 1$, into a pattern with wave number k and amplitude proportional to β. The other equation, Eq. (3), describes the evolution of an independent field $\Psi(x, t)$, which obeys the prototype model for spatiotemporal chaos, the Kuramoto-Sivashinsky model [2,3,5]. The inclusion in Eq. (2) of a term proportional to γ, which couples both equations, causes the pattern to exhibit chaotic spatiotemporal behaviors. The above model presents a coexistence region similar to that displayed by the LCLV experiment and the Lifshitz model; therefore, one expects the NK model to show chaoticon states.

In Fig. 5 we display the chaoticon and its respective spatiotemporal diagram obtained in the Lifshitz [Fig. 5(a)] and in the NK model [Fig. 5(b)]. The usefulness of the NK model is that the complex patterns are observed for small parameters ($\beta \ll 1$ and $\gamma \ll 1$) and analytical calculations, inaccessible in model (1), can be developed. Note, however, that the model (1) is the most simple one that describes the phenomena observed in the experiment. Moreover, it is an universal equation describing an instability and containing the essential ingredients for the emergence of localized chaotic spatiotemporal states.

In the phenomenological NK model, Eqs. (2) and (3), we can study the effect of the terms proportional to β and γ on the interaction of fronts between uniform states, where the upper state becomes spatiotemporally chaotic. Close to the Maxwell point ($\alpha \approx 0.5 + \Delta$), where Δ stands for the detuning from the Maxwell point, the NK model has motionless front solutions of the form $u_{\pm}(x) = 0.5 \pm 0.5\tanh(\sqrt{2}(x - \delta_0)/4)$, where δ_0 is the front position. From this solution, one can buildup a localized state which accounts for the effect of the spatiotemporal forcing

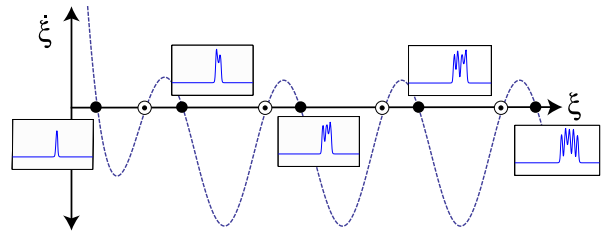

FIG. 6 (color online). Fronts interaction law accounting for the equilibrium chaoticon widths derived from Eq. (4). The closed (empty) circles represents stable (unstable) chaoticons.

(β and γ) and has the form $u(x, t) \approx [u_+(x - \delta_+(t)) + u_-(x - \delta_-(t)) - 1]$. By introducing the position $\chi \equiv (\delta_+ + \delta_-)/2$ and the width $\xi \equiv \sqrt{2}(\delta_+ - \delta_-)/4$ of the localized state, after straightforward calculations at the dominant order, we obtain

$$\dot{\chi} = A_1(t)\cos(k\chi)\cos(k\sqrt{2}\xi) + B_1(t)\sin(k\chi)\sin(k\sqrt{2}\xi),$$
$$\dot{\xi} = \frac{\Delta}{2} + be^{-\xi} + A_2(t)\cos(k\chi)\cos(k\sqrt{2}\xi) + B_2(t)\sin(k\chi)\sin(k\sqrt{2}\xi), \quad (4)$$

where $b \equiv 9\sqrt{2}/8$. The full and lengthy expressions of the other coefficients will be reported elsewhere. Briefly, $\{A_1(t), A_2(t), B_1(t), B_2(t)\}$ are formed by two parts, a constant term proportional to β and a chaotic term proportional to γ. The first equation describes the chaoticon position, which evolves chaotically in time around a given space location. From the second equation, we obtain the temporal evolution of the chaoticon width and we can derive the front interaction law. In Fig. 6 the width variation, corresponding to the force for an overdamped system, is plotted versus the width. Equilibrium points represent the chaoticon structures with different number of cells, from the smallest to the largest one.

The locking mechanism between the uniform state and the spatiotemporal chaotic pattern is due to the spatial periodic structure which induces a nucleation barrier in the front dynamics. A similar mechanism is observed in localized patterns [16,17], but the main difference is that the chaoticon interfaces maintain a chaotic dynamics around a given position. The dynamics described by Eqs. (4) qualitatively agree with the dynamics displayed by the Lifshitz model. However, in the NK model the chaotic behavior characterizes also small localized structures, at variance with those observed in the Lifshitz model and in the experiment.

In conclusion, spatiotemporal chaotic localized structures are reported in a LCLV experiment and numerical simulations of the model describing the system. Even though the comparison with the experimental observations is qualitative, the model allows grasping the essential ingredients of the phenomenon, namely, the coexistence between a uniform state and a spatially complex pattern

exists. A phenomenological model, where these ingredients are included, has allowed us to elucidate the front interaction mechanism that leads to the chaoticon structures. The extension of the mechanism in two dimensions remains an open problem.

We acknowledge financial support of the ANR international program, Project No. ANR-2010-INTB-402-02 (ANR-CONICYT39), "COLORS". M. G. C. thanks for the financial support of the FONDECYT Project No. 1120320. N. V. thanks the Master fellowship from CONICYT Contract No. 22111114 and the financial support of DPP of the University of Chile.

[1] G. Nicolis and I. Prigogine, *Self-Organization in Non Equilibrium Systems* (J. Wiley & Sons, New York, 1977).
[2] L. M. Pismen, *Patterns and Interfaces in Dissipative Dynamics*, Springer Series in Synergetics (Springer, Berlin, Heidelberg 2006).
[3] M. C. Cross and P. C. Hohenberg, Rev. Mod. Phys. **65**, 851 (1993).
[4] M. I. Rabinovich, A. B. Ezersky, and P. D. Weidman, *The Dynamics of Patterns* (World Scientific, Singapore, 2000).
[5] M. Cross, H. Greenside, *Pattern Formation and Dynamics in Nonequilibrium Systems* (Cambridge University Press, New York, 2009).
[6] P. Ball, *The Self-Made Tapestry: Pattern Formation in Nature* (Oxford University Press, New York, 1999).
[7] *Localized States in Physics: Solitons and Patterns*, edited by O. Descalzi, M. Clerc, S. Residori, and G. Assanto (Springer, New York, 2010).
[8] H. G. Purwins, H. U. Bodeker, and Sh. Amiranashvili, Adv. Phys. **59**, 485 (2010).
[9] P. L. Ramazza, E. Benkler, U. Bortolozzo, S. Boccaletti, S. Ducci, and F. T. Arecchi, Phys. Rev. E **65**, 066204 (2002).
[10] U. Bortolozzo, R. Rojas, and S. Residori, Phys. Rev. E **72**, 045201(R) (2005).
[11] F. Haudin, R. G. Elias, R. G. Rojas, U. Bortolozzo, M. G. Clerc, and S. Residori, Phys. Rev. Lett. **103**, 128003 (2009).
[12] T. Ackemann, W. J. Firth, and G. L. Oppo, Adv. At. Mol. Opt. Phys. **57**, 323 (2009).
[13] P. Coullet, Int. J. Bifurcation Chaos Appl. Sci. Eng. **12**, 2445 (2002).
[14] P. D. Woods and A. R. Champneys, Physica (Amsterdam) **129D**, 147 (1999).
[15] P. Coullet, C. Riera, and C. Tresser, Phys. Rev. Lett. **84**, 3069 (2000).
[16] M. G. Clerc and C. Falcon, Physica (Amsterdam) **356A**, 48 (2005).
[17] U. Bortolozzo, M. G. Clerc, C. Falcon, S. Residori, and R. Rojas, Phys. Rev. Lett. **96**, 214501 (2006).
[18] I. V. Barashenkov, E. V. Zemlyanaya, and T. C. van Heerden, Phys. Rev. E **83**, 056609 (2011).
[19] S. Fauve and O. Thual, Phys. Rev. Lett. **64**, 282 (1990).
[20] P. J. Martinez, L. M. Floria, F. Falo, and J. J. Mazo, Europhys. Lett. **45**, 444 (1999).
[21] N. V. Peskov, Computational Mathematics and Modeling **10**, 353 (1999).
[22] A. Kudrolli and J. P. Gollub, Phys. Rev. E **54**, R1052 (1996).
[23] M. G. Clerc, A. Petrossian, and S. Residori, Phys. Rev. E **71**, 015205(R) (2005).
[24] S. Residori, Phys. Rep. **416**, 201 (2005).
[25] F. Haudin, R. G. Elias, R. G. Rojas, U. Bortolozzo, M. G. Clerc, and S. Residori, Phys. Rev. E **81**, 056203 (2010).
[26] G. Kozyreff and M. Tlidi, Chaos **17**, 037103 (2007).
[27] F. Carbone, M. G. Clerc, and N. Verschueren (to be published).
[28] J. C. Sprott, *Chaos and Time-Series Analysis* (Oxford University Press, New York, 2003), p. 116; R. Deissler and K. Kaneko, Phys. Lett. A **119**, 397 (1987).
[29] J. D. Murray, *Mathematical Biology* (Springer-Verlag, Berlin, 1993).